High yield autoclave synthesis of pure $M_2B_{12}H_{12}$ (M=Na, K)

Jian Wang,[a] Timothy Steenhaut,[a] Hai-Wen Li,[b] Yaroslav Filinchuk,[a]*

[a] Institute of Condensed Matter and Nanosciences, Université Catholique de Louvain, 1348 Louvain-la-Neuve, Belgium

[b] Hefei General Machinery Research Institute, Hefei 230031, China

*Corresponding Author. E-mail: yaroslav.filinchuk@uclouvain.be (Y. Filinchuk)

Abstract

Metal dodecaborates ($M_xB_{12}H_{12}$) are a versatile class of materials used in polymer chemistry, cancer treatment and are promising candidates as electrolytes for solid-state batteries. However, a general and scalable approach has not yet been developed for producing high purity $B_{12}H_{12}^{2-}$ derivatives. In this work, we report a simple, efficient, and environmentally benign solvothermal method to prepare diffraction and ^{11}B NMR pure $Na_2B_{12}H_{12}$ (85 % yield) and $K_2B_{12}H_{12}$ (84 % yield). This new synthetic approach is based on the use of the borane dimethyl sulfide complex ($DMS{\cdot}BH_3$) and borohydrides ($NaBH_4$, KBH_4) heated at different temperatures in diglyme in an autoclave. It was found that high purity $Na_2B_{12}H_{12}{\cdot}$diglyme solvate is obtained via an intermediate formation of $B_3H_8^-$, $B_9H_{14}^-$, $B_{11}H_{14}^-$, which are all soluble in diglyme. Heating under vacuum is shown to be efficient to remove the coordinated diglyme, allowing to obtain unsolvated $Na_2B_{12}H_{12}$. Autoclave synthesis starting from KBH_4 directly yields solvent-free $K_2B_{12}H_{12}$, and ball-milling KBH_4 prior to the synthesis enabled to significantly improve the final yield. The new synthetic method paves the way to large-scale synthesis of $M_xB_{12}H_{12}$ derivatives, enabling to envisage a wider scope of practical applications.

Keywords: $Na_2B_{12}H_{12}$; $K_2B_{12}H_{12}$; Autoclave synthesis; Boron Chemistry

1. Introduction

Complex hydrides containing light elements are considered promising materials for solid-state hydrogen storage. Among these, metal borohydrides having high volumetric and gravimetric hydrogen densities, primarily $LiBH_4$, $Mg(BH_4)_2$ and $Ca(BH_4)_2$, [1-3] have attracted considerable attention. This includes reactive hydride composites with binary hydrides, such as $LiBH_4 + MgH_2$, which are capable to store hydrogen reversibly.[4] However, the major problem are the side reactions transforming BH_4^- anions into more stable dodecaborates, $B_{12}H_{12}^{2-}$, that cannot be easily rehydrogenated, therefore these compounds are often called "boron sinks" in this context.[5]

On the other hand, metal dodecaborates are interesting compounds as they find applications in cancer treatment, polymer chemistry and, more recently, as solid-state ionic conductors.[6-11] They contain closed icosahedral boron clusters with twelve terminal hydrogen atoms in each corner (As shown in Figure 1), and have a remarkable chemical and thermal stability.[12, 13] However, dodecaborates, such as $Li_2B_{12}H_{12}$ and $Na_2B_{12}H_{12}$, are commercially available, but at a very high price (e.g. 5 g of $Na_2B_{12}H_{12}$ cost around 600 €).[14] Investigation of the sizeable scale synthesis of $M_xB_{12}H_{12}$ has therefore been subject to a great effort of many research groups over the past decades.

The $B_{12}H_{12}^{2-}$ anion was first obtained by Hawthorn in 1960, in very low yields as byproduct of the reaction between triethylamine and 2-iododecaborane in benzene.[15] Since then, synthetic methods for obtaining dodecaborate salts have been continuously developed and improved.[13, 16-18] However, these methods still suffer from low yields or the use of toxic and flammable boranes (B_2H_6 and $B_{10}H_{14}$) as precursors. The main synthetic methods developed so far are based on two types of reactions.

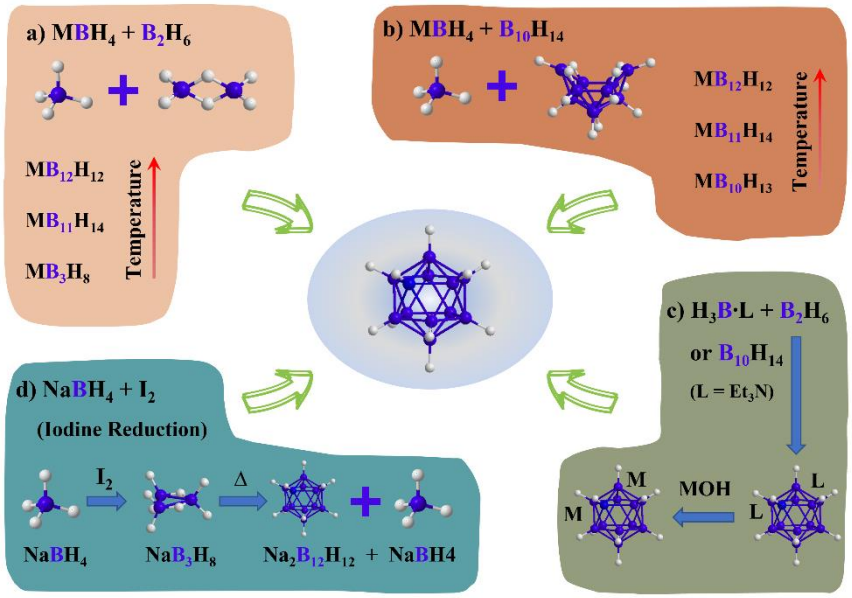

Figure 1. Schematic of known synthesis routes for metal $B_{12}H_{12}^{2-}$.

The first method is the reaction of borohydrides with boranes (B_2H_6 or $B_{10}H_{14}$), that produces a series of boron-rich anions (Figure 1a and b). The reaction between B_2H_6 and $NaBH_4$ in triethylamine at room temperature leads to the formation of NaB_3H_8 with a higher yield than the method described above. By rising the temperature to 180 °C, $Na_2B_{12}H_{12}$ is obtained in a high yield of around 90 %. Below this temperature, lower borane anions, such as $B_{11}H_{14}^-$, are formed instead.[19] Generally, higher temperatures favor the formation of B–B bonds, forming polyhedral boranes that tend to become larger and more stable with increasing reaction temperatures.[20] Solvent-free methods, like annealing in sealed tubes, were employed for the reaction between solid state decaborane ($B_{10}H_{14}$) and borohydrides. However, in this case, the reaction leads to the formation of $B_{12}H_{12}^{2-}$ together with other B−H compounds.[17, 21] The $B_{12}H_{12}^{2-}$ anion can also be formed by the reaction between boranes (B_2H_6 or $B_{10}H_{14}$) and borane triethylamine complex precursors (shown in Figure 1c).[19, 20] Since nowadays green chemistry is gaining attention for chemical syntheses, the use of toxic and expensive compounds such as B_2H_6 and $B_{10}H_{14}$ should be avoided whenever possible.

The second method is a two-step synthesis that relies on the oxidation of borohydrides by iodine (Scheme 1).[16, 22] During the first step, $NaBH_4$ reacts with I_2 in diglyme (diethylene glycol dimethyl ether), giving NaB_3H_8 as main intermediate.

$Na_2B_{12}H_{12}$ can then be obtained as one of the pyrolysis products of NaB_3H_8, at 150 °C (equation 1 and 2). This route can be made cheap and specific, but the yield is not high (between 50 and 60 %) due to low conversion of $NaBH_4$ and the difficulty of the purification process.

$$3\ NaBH_4 + I_2 \rightarrow NaB_3H_8 + 2\ NaI + 2\ H_2 \quad (1)$$

$$5\ NaB_3H_8 \rightarrow Na_2B_{12}H_{12} + 3\ NaBH_4 + 8\ H_2 \quad (2)$$

Scheme 1. Synthesis of $Na_2B_{12}H_{12}$ by oxidation of sodium borohydride with iodine and subsequent pyrolysis of the formed NaB_3H_8 intermediate.

In this study, we propose a new and convenient route for the one pot synthesis of sodium and potassium dodecaborates from their respective borohydrides and the borane dimethyl sulfide complex ($DMS{\cdot}BH_3$) in an autoclave. The use of an autoclave does not only provide an enclosed system to keep all gaseous species confined, but also enables increasing the boiling point of diglyme, which is used as solvent, hence increasing the solubility of the used borohydrides. We firstly investigated the effect of reaction temperature on the synthesis exploiting sodium as cation.

Previous research showed that diglyme is easily chelated with dodecaborate salts with smaller cations, such as Na^+ and Li^+.[23] To obtain non-solvated dodecaborates with those cations, synthesis can be undertaken with larger monovalent cations such as trimethylammonium, yielding water-insoluble products ($[(CH_3)_3NH]_2B_{12}H_{12}$) with no coordinating diglyme. $Na_2B_{12}H_{12}$ can then be obtained by simple cation exchange between $[(CH_3)_3NH]_2B_{12}H_{12}$ and NaOH in water.[18] For the present work, desolvation of diglyme by thermal treatment from the obtained diglyme-solvated $Na_2B_{12}H_{12}$ was studied. Once optimized for the sodium derivative, the method was further developed to obtain $K_2B_{12}H_{12}$ from KBH_4 and $DMS{\cdot}BH_3$. All the obtained samples were characterized by means of powder X-ray diffraction (PXRD), and Fourier-transform infrared, nuclear magnetic resonance and inductively coupled plasma optical emission spectroscopies (FTIR, NMR and ICP-OES). Their thermal properties were assessed by thermal gravimetric and differential scanning calorimetric (TGA/DSC) methods.

2. Experimental Section

2.1. Chemicals

Sodium borohydride ($NaBH_4$, anhydrous, 95 %), potassium borohydride (KBH_4, anhydrous, 98 %), Borane triethylamine complex ($(C_2H_5)_3N{\cdot}BH_3$, 97%), borane dimethyl sulfide complex ($(CH_3)_2S{\cdot}BH_3$, analytical) and diethylene glycol dimethyl ether (diglyme, $C_6H_{14}O_3$, anhydrous, 99.5%) were obtained from Sigma-Aldrich. Deuterated dimethyl sulfoxide (DMSO-d_6, anhydrous, 99.9 atom % D) was obtained from Eurisotop. All the above chemicals were used without further purification. Commercial $Na_2B_{12}H_{12}$ (99.5%) was purchased from Katchem and was dried at 150 °C under vacuum for 2 h before PXRD and FTIR measurements.

2.2. General Synthetic Procedure

The reaction was performed in a 37.5 mL quartz liner fitted inside a stainless steel autoclave (Anhui Kemi Instrument Co., Ltd., the volume of the autoclave is 50 mL, Figure S1). Typically, 0.19 g $NaBH_4$ (5 mmol, or 0.27g KBH_4) was weighted into the quartz liner reactor in a glovebox and the glass reactor was sealed by Parafilm. Before loading the quartz reactor into the autoclave, 16 mL of diglyme (the solubility of $NaBH_4$ in diglyme at room temperature is reported to be 0.55 g/g),[24] and subsequently 27.5 mmol of borane dimethyl sulfide complex $(CH_3)_2S{\cdot}BH_3$ (2.75 mL) were added to the borohydride. The autoclave was then sealed and the system purged with argon for 30 s to remove air in the system, and the solution was then stirred further at room temperature for another 10 min. The reaction temperature was controlled by a programmed system and was increased at a heating rate of 2 °C/min from RT to the final reaction temperature, at which it was maintained for 24 h. Subsequently, the system was naturally cooled down to room temperature. The reaction mixture was then filtered, using a Schlenk filtration apparatus (Figure S2), and washed with diglyme (3x10 mL), followed by drying at 80 °C under vacuum for 2h to transform sticky powders into dry ones for PXRD and ATR-FTIR measurements. The raw product was obtained as a white substance. The desolvated samples were obtained by heating at 200 °C or 150 °C under vacuum for 12 h.

In this work, different temperatures were investigated for both reaction and desolvation. The obtained samples were labelled as MD-X-Y, where M = alkali ion (Na

or K) and D was the abbreviation of $DMS{\cdot}BH_3$, X stands for the reaction temperature (in °C, ranging from 90 to 200 °C) and Y denotes the desolvation temperature (in °C, either 150°C or 200 °C). The raw product was obtained as a white solid substance.

Purified $K_2B_{12}H_{12}$ was obtained by refluxing samples in boiling demineralized water (100 °C, 1h). Samples were then filtrated and dried at 120 °C under vacuum for 4 h.

Ball milled KBH_4 (bm-KBH_4) was produced by mechanical milling of 0.5g KBH_4 at room temperature using a planetary ball mill (Fritsch Pulverisette P7) upon loading with 4 steel balls (10 mm in diameter) in a hardened steel vials (30 cm^3 in volume) in an argon-filled glovebox. Milling was performed under 0.1 MPa of Ar for 2 h (2 min milling cycles, 3 min pausing, 24 cycles).

2.3. Characterization

2.3.1. Powder X-ray Diffraction (PXRD)

Powder X-ray diffraction (PXRD) patterns were collected using a MAR 345 image plate detector, utilizing Mo Kα radiation (λ = 0.71073 Å) from and Incoatec Microfocus Source Mo ELM47 operating at 50 kV and 1000 μA. Samples were rotated 180° during exposure for 10 minutes. Samples were loaded into thin-walled glass capillaries (0.7 mm diameter, Hilgenberg, GmbH) under argon in a glovebox. The capillaries were sealed with grease in the glovebox. Once removed from the glovebox, they were cut and immediately placed into molten wax on goniometric heads and measured immediately after preparation to avoid sample degradation. Data were integrated by the Fit2D software (ESRF), using LaB_6 as calibrant.

2.3.2. TGA/DSC analyses

TGA/DSC analysis was performed on NETZSCH STA 449 F3 Jupiter instrument equipped with a stainless steel oven, housed inside an argon-filled glovebox. Measurements were performed at a heating rate of 5 K/min under constant Ar flow (total flow of 100 mL/min), from 25 to 500 °C.

2.3.3. FTIR analysis

The attenuated total reflectance Fourier transform infrared (ATR-FTIR) spectra were measured on a Bruker Alpha II spectrometer set in an argon-filled glovebox. For

the measurements, the spectrometer was equipped with a Platinum ATR module (Bruker, diamond crystal, single bounce).

2.3.4. NMR Spectroscopy

All NMR spectra were recorded at room temperature (295 K) on a Bruker Avance 500 spectrometer operating at 500.13 MHz for ^{1}H and 160.46 MHz for ^{11}B, using a BBFO {^{1}H, X} probehead equipped with a *z*-gradient coil. Experiments were run under the *TopSpin* program (1.3 version; Bruker). ^{1}H chemical shifts were referenced to the residual DMSO-d_5 signal (δ = 2.50 ppm) and ^{11}B NMR signals were referenced externally to $BF_3 \cdot Et_2O$ (δ = 0.00 ppm). All experiments were conducted using quartz NMR tube (internal diameter = 5 mm)

2.3.5. ICP-OES

ICP-OES analyses were carried out on an ICAP-6500 apparatus from ThermoFisher Scientific, upon dissolution of the samples in purified water.

3. Results and Discussion

3.1. Influence of the reaction temperature on the reaction products in the synthesis of

$Na_2B_{12}H_{12}$·diglyme

Borane complexes have proven exceedingly useful for hydroboration reactions. They offer similar reactivity to diborane (B_2H_6) but have fewer storage and handling issues. Among available complexes, borane tetrahydrofuran complex (THF·BH_3), borane triethylamine complex (Et_3N·BH_3) and DMS·BH_3 are the most popular agents. Although THF·BH_3 is more reactive than DMS·BH_3 and Et_3N·BH_3, it is commercially available only as a solution in THF. In contrast, DMS·BH_3 and Et_3N·BH_3 are more stable and readily available as neat reagents. However, Et_3N·BH_3 has a million times lower dissociation constant than DMS·BH_3.[25] This is the reason of its lower reactivity with borohydrides: indeed, we observed in our first experimental attempts that $NaBH_4$/KBH_4 and Et_3N·BH_3 at 180 °C in an autoclave did not yield any dodecaborates. Hence, we focused on using DMS·BH_3 in the reaction with $NaBH_4$, studying the effect of the reaction temperature (90, 120, 160 and 200 °C) on the obtained products. Once the reaction was completed in an autoclave, the products were initially dried at 80 °C, transforming sticky powders into dry samples, i.e. removing most of the free diglyme and allowing to characterize the samples easily. Figure 2 depicts the proton coupled ^{11}B NMR spectra of as-prepared NaD-X-80 (X=120, 160 and 200) samples. Reaction at a temperature of 90 °C (sample NaD-90-80) did not lead to the formation of any solid precipitate. The NMR spectrum of the reaction solution of NaD-90-80 (Figure S3) shows that mainly $B_3H_8^-$ was formed, together with some boron clusters with higher nuclearity ($B_9H_{14}^-$ and $B_{11}H_{14}^-$), which are all soluble in diglyme.[22, 25, 26] This is consistent with earlier reports of the formation of $B_9H_{14}^-$ and $B_{11}H_{14}^-$ by dehydrocondensation of $B_3H_8^-$ with diborane in diglyme at low temperatures around 70 to 90 °C.[25] When higher reaction temperatures are used (120 and 160°C), solid precipitates appeared after cooling the autoclave. ^1H-coupled ^{11}B NMR spectra of NaD-120-80 and NaD-160-80 dissolved in DMSO-d_6 show doublet peaks at approximately -15 ppm, which indicate the presence of $B_{12}H_{12}^{2-}$. The ^{11}B NMR spectra do not show the formation of any other solid boron compounds under those reaction conditions.[13, 26] For NaD-200-80, an additional multiplet is present at -17.2 ppm, partly overlapping the doublet of $B_{12}H_{12}^{2-}$. It can be assigned to $B_{11}H_{11}^{2-}$, likely forming due

to the decomposition of intermediates, such as $B_{11}H_{14}^-$, at high temperatures, as indicated by previous works.[9] These results show that temperature is a crucial factor for the outcome of the synthesis, as it usually is for the synthesis of polyhedral borates.

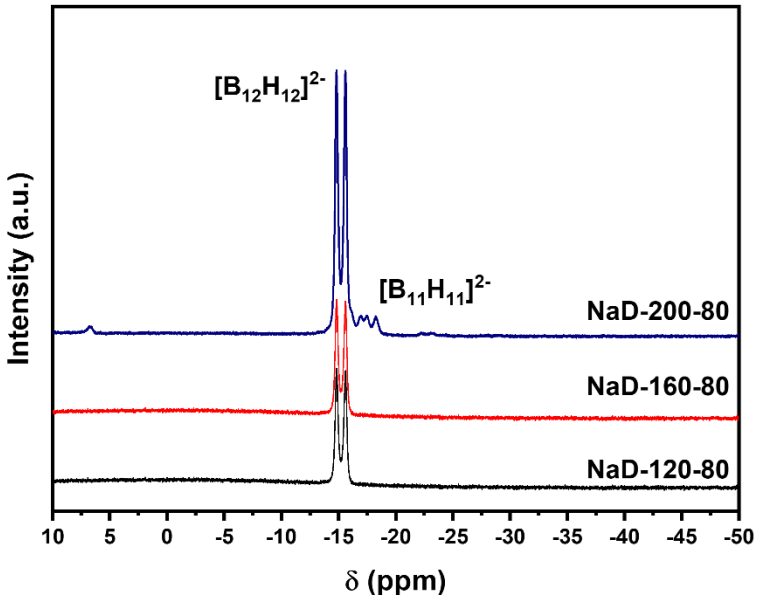

Figure 2. ^{1}H-coupled ^{11}B NMR spectra of the solid precipitates formed in the reaction conditions used for NaD-X-80 (X = 120; 160; 200). Measurements were performed on samples dissolved in DMSO-d_6.

TGA/DSC analyses were performed to investigate the thermal stability and composition of the NaD-X-80 (X=120, 160, 200) samples, which were compared to commercial $Na_2B_{12}H_{12}$. Figure 3(a) shows that commercial $Na_2B_{12}H_{12}$ displays an endothermic signal on the DSC curve, accompanied by a small mass loss of about 1 wt. % on TGA, around 100 °C, which is ascribed to the loss of physically adsorbed water. The DSC curve furthermore shows an endothermic peak with a maximum at 266°C, without mass loss, which is explained by a well-known phase transition of $Na_2B_{12}H_{12}$.[27] For the synthesized samples, the loss of some diglyme can be observed from DSC curves, starting around 110 °C. The DSC curves of all the synthesized samples show an intense endothermic peak around 142 °C, accompanied by a weight loss, attributed to the liberation of the remaining coordinated diglyme. A separate experiment consisting of drying the sample at 150 °C under vacuum was performed, showing that the PXRD pattern (Figure S4) has changed upon this treatment, which confirms that the weight loss is due to the departure of diglyme inside the structure. A similar endothermic peak and weight loss are also present around 201°C, which is

attributed to the release of the coordinated diglyme, that is known to form chelates with small cations such as Na^+ and Li^+.[23]

The DSC curve of NaD-120-80 shows the typical endothermic peak related to the phase transition of the solvent-free $Na_2B_{12}H_{12}$ at 266 °C (Figure 3b), in agreement with the behavior of the commercial sample. This phase transition peak is however not observed on the DSC curves of NaD-160-80 and NaD-200-80. XRD data (Figure 5) shown below indicate that solvated $Na_2B_{12}H_{12}$ obtained at 120 °C has a different structure than products obtained at higher synthesis temperatures (160 °C). The decomposition of the high temperature (HT) form of $Na_2B_{12}H_{12}$·diglyme likely leads directly to the HT form of $Na_2B_{12}H_{12}$, thus explaining the absence of the DSC peak at 266 °C. In addition, a new endothermic peak at 220 °C is observed on the DSC curve of NaD-200-80, which is due to the desolvation of $Na_2B_{11}H_{11}$·diglyme that is present as a secondary product.

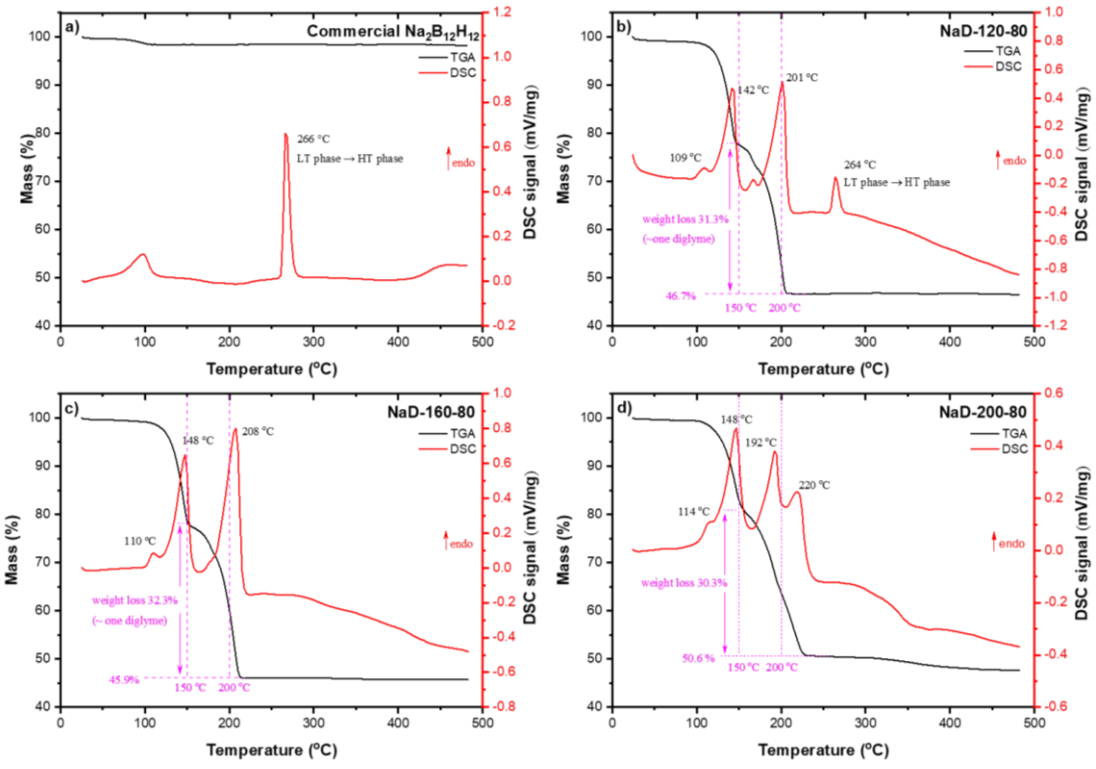

Figure 3. TGA-DSC curves of (a) commercial $Na_2B_{12}H_{12}$ and (b,c and d, respectively) NaD-X-80 (X=120, 160, 200) samples, measured under argon, with a heating rate of 5 K/min from RT to 500 °C.

3.2. Removal of diglyme from $Na_2B_{12}H_{12}$·diglyme

Based on the results of the TGA-DSC experiments, we decided to investigate

drying temperatures of 150 °C and 200 °C in order to obtain desolvated $Na_2B_{12}H_{12}$. The solvent removal was performed in a Schlenk flask connected to a vacuum pump, and the obtained dried samples were analysed by FTIR (Figure 4) and PXRD (Figure 5). Typical signals of the $B_{12}H_{12}^{2-}$ anion are observed for all samples; 1074 cm^{-1} (vibration of B−B bond), 2467 cm^{-1} (B−H symmetric and antisymmetric stretchings), 713 and 539 cm^{-1} (B−H bending and rocking vibrations).[18] The absorption bands located at 3000−2750 cm^{-1} and 1500−1300 cm^{-1} present in the spectra of the sample dried at 80 °C are attributed to C−H and C−O stretching mode of diglyme, respectively. The disappearance of these bands from the FTIR spectrum upon drying the samples at 200 °C proves that this temperature enables an effective removal of all the coordinated diglyme.

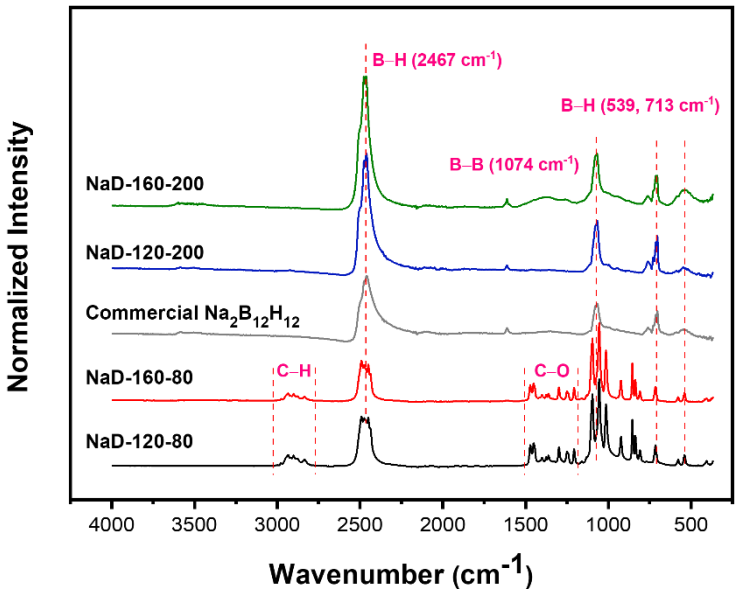

Figure 4. FTIR spectra of NaD-X-Y (X=120, 160; Y=150, 200) samples.

All samples before and after drying were analyzed with PXRD. As shown in Figure 5, the PXRD patterns of the as-prepared NaD-120-200 and NaD-160-200 are in good agreement with the commercial $Na_2B_{12}H_{12}$, having a monoclinic $P2_1/n$ structure corresponding to the low temperature (LT) phase (ICSD 164649). A peak shift and broadening are observed for the NaD-160-200 sample in the zoomed diffraction pattern (Figure 5b). All patterns were measured under the same conditions, and the observed shift and broadening can likely be attributed to a higher number of structural defects resulting from the higher reaction temperature. The solvated samples, obtained by

drying the reaction products at 80 °C and 150 °C, show very different diffraction patterns (Figure S4), indicating that the diglyme-solvated $Na_2B_{12}H_{12}$ phases corresponding to NaD-120-80 and NaD-160-80 are not the same.

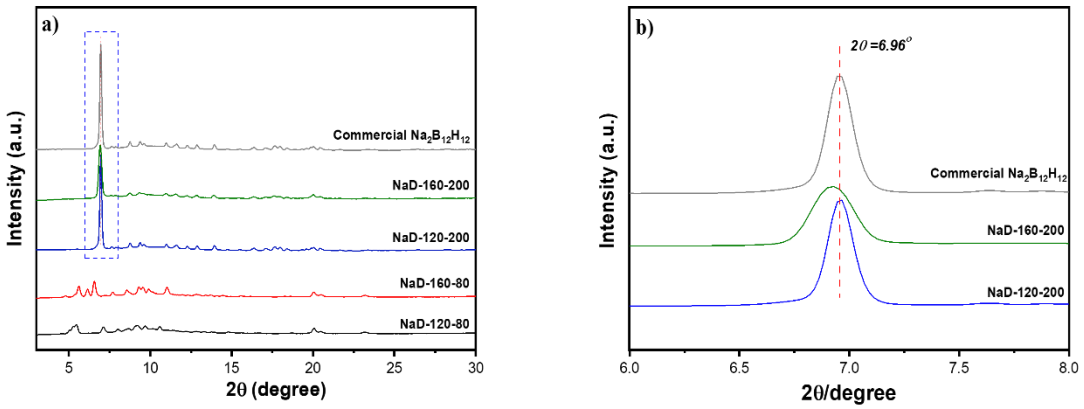

Figure 5. a) PXRD patterns of the NaD-X-Y (X=120, 160; Y=150, 200) samples; b) zoom between 6 and 8 degrees.

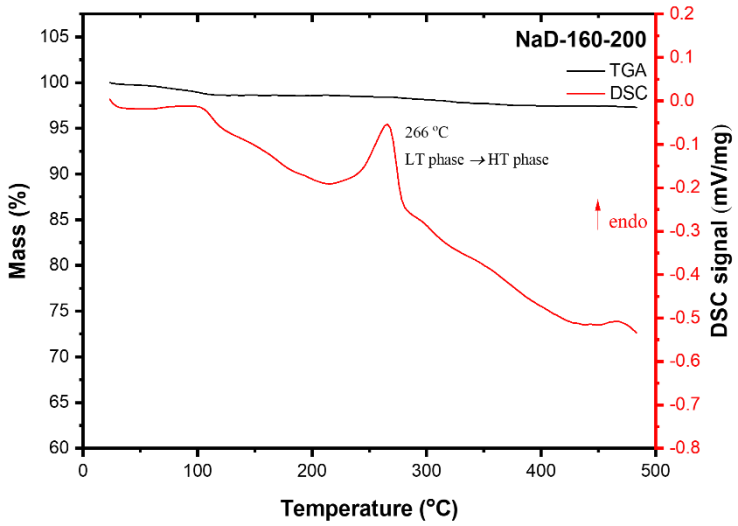

Figure 6. TGA/DSC analysis of NaD-160-200, measured under argon, with a heating rate of 5 K/min from RT to 500 °C.

The desolvated NaD-160-200 was further characterized by ICP-OES. As shown in Table S1, the experimentally determined Na/B ratio is in very good agreement with the expected value for $Na_2B_{12}H_{12}$. Figure 6 shows the TGA and DSC curves for the same sample. The total weight loss is about 2.5 % on heating from room temperature to 500 °C, including the weight loss below 110°C due to the departure of physically absorbed water. The gradual and small weight loss after 150 °C is ascribed to the removal of the remaining traces of diglyme. This residual diglyme (~2 mol %) was also

observed in the ^{1}H NMR spectrum (Figure S6). The DSC curve shows a remarkable endothermic peak at 264°C, characteristic for the LT to HT phase transition of $Na_2B_{12}H_{12}$. The yield of desolvated $Na_2B_{12}H_{12}$ is calculated as being 85 % for NaD-160-200, and 72 % for NaD-120-200.

Our synthesis likely follows the equation with the following stoichiometry (eq. 3):

$$2\ NaBH_4 + 10\ (CH_3)_2S{\cdot}BH_3 \rightarrow Na_2B_{12}H_{12} + 10\ (CH_3)_2S + 13\ H_2 \quad (3)$$

This equation is consistent with the amount of formed gas measured by the pressure build up in the autoclave once it is cooled down to room temperature, see Table S2. The mechanism of the reaction most likely involves as the first step the formation of $B_3H_8^-$ (eq. 4):

$$BH_4^- + 2\ BH_3 \rightarrow B_3H_8^- + H_2 \quad (4)$$

This reaction pathway has previously been demonstrated for the synthesis of alkali metal octohydrotriborate salts,[28, 29] with an excess of $(CH_3)_2S{\cdot}BH_3$ being advantageous in improving the yield of $B_3H_8^-$. This first step would then be followed by the condensation of $B_3H_8^-$ with $(CH_3)_2S{\cdot}BH_3$ to form $B_{12}H_{12}^{2-}$ (eq. 5):

$$2\ B_3H_8^- + 6\ BH_3 \rightarrow Na_2B_{12}H_{12\ (LT\text{-}phase)} + 11\ H_2 \quad (5)$$

At temperatures above 120 °C, other boranes are also produced. $(CH_3)_2S{\cdot}BH_3$ is in equilibrium with B_2H_6, known to undergo pyrolysis.[29] Indeed, for NaD-120-200, the reaction is dominated by the dehydrocondensation of BH_4^- by BH_3. An increased yield of $Na_2B_{12}H_{12}$ is observed only when the synthesis is performed at higher temperature, namely 160 °C, leading to the decomposition of NaB_3H_8 according to eq. 2.[18] $Na_2B_{12}H_{12}$ and $NaBH_4$ are formed during the decomposition of NaB_3H_8, and the newly formed $NaBH_4$ is recycled into NaB_3H_8 by reacting with the remaining $DMS{\cdot}BH_3$, subsequently transforming into $Na_2B_{12}H_{12}$. The involved reactions can be described as follows:

$$BH_4^- + 2\ BH_3 \rightarrow B_3H_8^- + H_2 \quad (6)$$

$$5\ NaB_3H_8 \rightarrow Na_2B_{12}H_{12\ (HT\ phase)} + 3\ NaBH_4 + 8\ H_2 \quad (7)$$

3.3. Synthesis of $K_2B_{12}H_{12}$

Since the synthesis worked well for the sodium salt, we further optimized the procedure for obtaining $K_2B_{12}H_{12}$. Despite the solubility of KBH_4 in diglyme is low, the

yield of $K_2B_{12}H_{12}$ by using our approach reached 84%, and actually the real yield is even higher, as $K_2B_{12}H_{12}$ is slightly soluble in diglyme not enabling full recovery of the formed product. On the other hand, K^+ has a lower charge density than Na^+ and is less frequently coordinating with diglyme in solid state, allowing to obtain unsolvated $K_2B_{12}H_{12}$ upon drying at only 150 °C under vacuum.[23] The synthesis of $K_2B_{12}H_{12}$ was carried out at 120 °C and 200 °C. We also used ball-milled KBH_4 as reactant, as it enables higher contact surface with the solution during synthesis. Figure S5 shows the PXRD pattern of commercially supplied KBH_4 and ball-milled KBH_4, the peak intensities and widths are the same. The size reduction by ball milling is clearly revealed by optical microscopy (Figure S7), showing that the procedure is efficient. ball milling is effective in reducing the size of KBH_4; the difference is not visible in PXRD patterns, as the long-range ordered of the crystal structure is not affected by ball milling.

Figure 7 shows the ^{11}B NMR spectra and ^1H NMR patterns of the obtained samples upon drying at 150 °C (KD-X-150), synthesized by reacting $DMS{\cdot}BH_3$ with either commercially supplied KBH_4, or ball-milled KBH_4. The yields of $K_2B_{12}H_{12}$ are summarized in Table S3 and Table S4. The NMR spectra clearly show that non-milled KBH_4 mainly converts into $K_2B_{12}H_{12}$, although there is a small amount of KBH_4 remaining upon reaction (about 11 wt. % for reaction at 120 °C). The bm-KD-120-150 sample showed a much higher yield and purity (97 %) than KD-120-150 (89 %). This indicates that larger contact surface of KBH_4 particles leads to improved reaction between KBH_4 and $DMS{\cdot}BH_3$. With increasing reaction temperatures, the yields of $K_2B_{12}H_{12}$ also significantly increase, demonstrating again that temperature plays a key role in the formation of B−B bonds. The ^1H NMR spectrum (Figure 7b) showed a similar tendency with ^{11}B NMR spectra

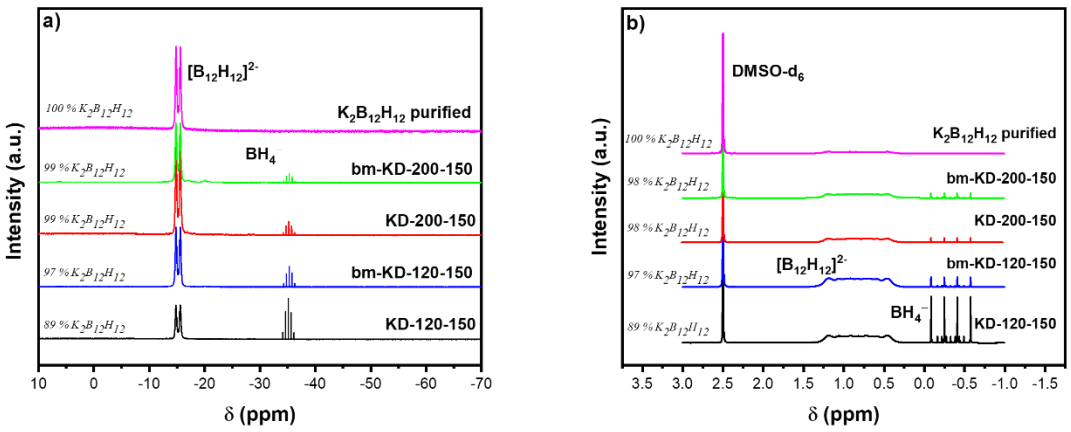

Figure 7. a) ^{11}B NMR and b) ^{1}H NMR spectra of synthesized KD-X-150 (X=120; 200) samples, purities of $K_2B_{12}H_{12}$ are calculated from ^{11}B NMR peak integration

Figure 8 shows the PXRD patterns of the KD-X-150 (bm-KD-X-150) samples and $K_2B_{12}H_{12}$ purified by refluxing in hot water (see experimental section). The PXRD patterns clearly show the presence of $K_2B_{12}H_{12}$ (COD 1533614) and KBH_4 as only diffracting phases in the as-synthesized samples. For the sample purified in water, $K_{12}B_{12}H_{12}$ is the only phase present, demonstrating that this purification approach is efficient.

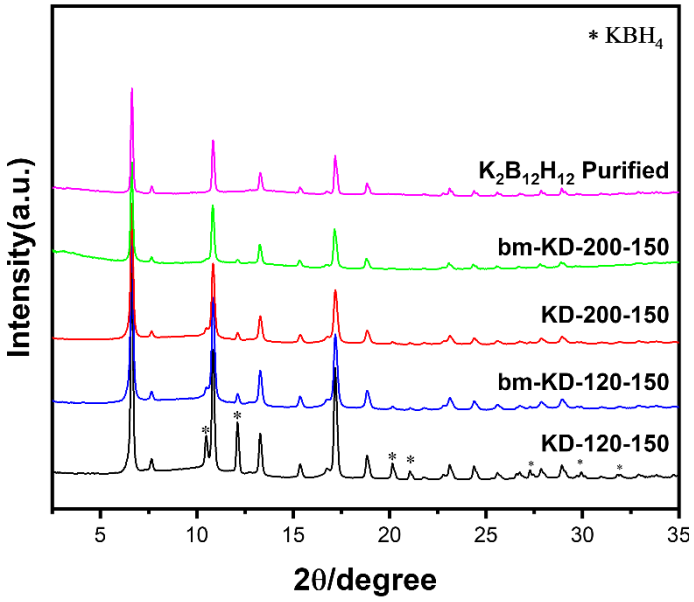

Figure 8. PXRD patterns of as-synthesized $K_2B_{12}H_{12}$ samples.

Conclusion

We demonstrated a new solvothermal synthesis method for obtaining high purity $Na_2B_{12}H_{12}$ and $K_2B_{12}H_{12}$. This new approach is based on the reaction between the corresponding alkali borohydrides and the $DMS{\cdot}BH_3$ complex in diglyme in an autoclave. The solubility of the borohydrides increases with temperature thus leading to a higher yield of $B_{12}H_{12}^{2-}$: the best conditions for $Na_2B_{12}H_{12}$ synthesis are at 160°C (85% yield), and 200 °C for $K_2B_{12}H_{12}$(84% yield), producing X-ray and ^{11}B NMR pure samples. Lower temperatures led to incomplete conversion of $NaBH_4$ into $Na_2B_{12}H_{12}$, attributed to the formation of diglyme-soluble species such as $B_3H_8^-$, $B_9H_{14}^-$, $B_{11}H_{14}^-$, whereas higher temperatures led to the formation of various impurities, including $B_{11}H_{11}^{2-}$. Moreover, the different reaction temperatures lead to the formation of different diglyme-solvated $Na_2B_{12}H_{12}$ phases. When using temperatures higher than 160 °C, the final desolvated product contains a higher number of structural defects. Desolvation of $Na_2B_{12}H_{12}{\cdot}$diglyme is efficient in vacuum at 200 °C. Since KBH_4 is insoluble in diglyme, reducing the particle size of KBH_4 by ball-milling allows to increase the yields of $K_2B_{12}H_{12}$. The temperature was shown to also have a crucial importance, similarly to the synthesis of $Na_2B_{12}H_{12}$. $K_2B_{12}H_{12}$ presents some solubility in diglyme; the totality of the formed product is thus not recovered in the precipitate, but the mother liquor may be recycled for a subsequent batch to further increase the yield. The new method that we developed for the synthesis of $Na_2B_{12}H_{12}$ and $K_2B_{12}H_{12}$ presents an important improvement compared to previous strategies that are more difficult to implement and usually lead to lower yields and higher production costs.

AUTHOR INFORMATION

Notes

The authors declare no competing financial interest.

ACKNOWLEDGMENT

This work was financially supported by China Scholarship Council (201806930031), and the FNRS (PDR T.0169.13, EQP U.N038.13, J.0164.17, CdR J.0073.20) and the Communauté Française de Belgique under Grant ARC 18/23-093. The authors acknowledge Anne Iserentant for the ICP-OES measurements.

ASSOCIATED CONTENT

Supporting information

Schemes of high-pressure autoclave used for the synthesis of $[B_{12}H_{12}]^{2-}$ and complete Schlenk line setup; ^{1}H coupled ^{11}B NMR spectra of synthesized NaD-90-80; PXRD Patterns of NaD-X-150 samples; ICP-OES analysis results of NaD-160-200*;* PXRD patterns of commercial KBH_4 and ball milled KBH_4; Optical microscopy images of commercial KBH_4 and ball-milled KBH_4; ^{1}H NMR spectrum of NaD-160-200; Pressures observed during autoclave experiments; Side-product identification and yields of $K_2B_{12}H_{12}$ obtained under different reaction conditions; ^{1}H NMR spectrum of purified $K_2B_{12}H_{12}$.

References

1. Li, H.-W.; Yan, Y.; Orimo, S.-i.; Züttel, A.; Jensen, C. M., Recent Progress in Metal Borohydrides for Hydrogen Storage. *Energies* **2011,** *4* (1), 185-214.

2. Paskevicius, M.; Jepsen, L. H.; Schouwink, P.; Černý, R.; Ravnsbæk, D. B.; Filinchuk, Y.; Dornheim, M.; Besenbacher, F.; Jensen, T. R. Metal Borohydrides and Derivatives – Synthesis, Structure and Properties *Chem. Soc. Rev.* **2017**, 46, 1565– 1634.

3. Milanese, C.; Jensen, T. R.; Hauback, B. C.; Pistidda, C.; Dornheim, M.; Yang, H.; Lombardo, L.; Zuettel, A.; Filinchuk, Y.; Ngene, P.; de Jongh, P. E.; Buckley, C. E.; Dematteis, E. M.; Baricco, M., Complex hydrides for energy storage. *Int. J. Hydrogen Energy* **2019,** *44* (15), 7860-7874.

4. Jepsen, J.; Milanese, C.; Girella, A.; Lozano, G. A.; Pistidda, C.; Bellosta von Colbe, J. M.; Marini, A.; Klassen, T.; Dornheim, M., Compaction pressure influence on material properties and sorption behaviour of $LiBH_4$–MgH_2 composite. *Int. J. Hydrogen Energy* **2013,** *38* (20), 8357-8366.

5. Grahame, A.; Aguey-Zinsou, K.-F., Properties and Applications of Metal (M) dodecahydro-closo-dodecaborates ($Mn=_{1,2}B_{12}H_{12}$) and Their Implications for Reversible Hydrogen Storage in the Borohydrides. *Inorganics* **2018,** *6* (4).

6. He, L.; Li, H.-W.; Nakajima, H.; Tumanov, N.; Filinchuk, Y.; Hwang, S.-J.; Sharma, M.; Hagemann, H.; Akiba, E., Synthesis of a Bimetallic Dodecaborate $LiNaB_{12}H_{12}$ with Outstanding Superionic Conductivity. *Chem. Mater.* **2015,** *27* (16), 5483-5486.

7. Barth, R. F.; Mi, P.; Yang, W., Boron delivery agents for neutron capture therapy of cancer. *Cancer Commun (Lond)* **2018,** *38* (1), 35.

8. Li, J.; Janouskova, O.; Fernandez-Alvarez, R.; Mesikova, S.; Tosner, Z.; Kereiche, S.; Uchman, M.; Matejicek, P., Designed Boron-Rich Polymeric Nanoparticles Based on Nano-ion Pairing for Boron Delivery. *Chemistry* **2020,** *26* (63), 14283-14289.

9. Gigante, A.; Duchene, L.; Moury, R.; Pupier, M.; Remhof, A.; Hagemann, H., Direct Solution-Based Synthesis of Na_4 (B_{12} H_{12})(B_{10} H_{10}) Solid Electrolyte. *ChemSusChem* **2019,** *12* (21), 4832-4837.

10. Guzik, M. N.; Mohtadi, R.; Sartori, S. Lightweight Complex Metal Hydrides for Li-, Na-, and Mg-Based Batteries. *J. Mater. Res.* **2019**, 34 (6), 877– 904.

11. Brighi, M.; Murgia, F.; Černý, R. Closo-Hydroborate Sodium Salts as an Emerging Class of Room-Temperature Solid Electrolytes. Cell Reports Phys. Sci. 2020, 1 (10), 100217.

12. Yan, Y.; Remhof, A.; Rentsch, D.; Zuttel, A., The role of $MgB_{12}H_{12}$ in the hydrogen desorption process of $Mg(BH_4)_2$. *Chem. Commun. (Camb)* **2015,** *51* (4), 700-2.

13. Moury, R.; Gigante, A.; Hagemann, H. An Alternative Approach to the Synthesis of NaB_3H_8 and $Na_2B_{12}H_{12}$ for Solid Electrolyte Applications. *Int. J. Hydrogen Energy* 2017, 42, 22417– 22421.

14. Katchem. http://www.katchem.cz.

15. Pitochelli, A. R.; Hawthorne, F. M. The Isolation of The Icosahedral $B_{12}H_{12}^{-2}$ Ion. *J. Am. Chem. Soc.* **1960**, 82, 3228-3229.

16. Geis, V.; Guttsche, K.; Knapp, C.; Scherer, H.; Uzun, R., Synthesis and characterization of synthetically useful salts of the weakly-coordinating dianion $[B_{12}Cl_{12}]^{2-}$. *Dalton Trans* **2009,** (15), 2687-94.

17. He, L.; Li, H.-W.; Tumanov, N.; Filinchuk, Y.; Akiba, E. Facile Synthesis of Anhydrous Alkaline Earth Metal Dodecaborates $MB_{12}H_{12}$ (M = Mg, Ca) from $M(BH_4)_2$ *Dalton Trans.* 2015, 44, 15882–15887.

18. Pylypko, S.; Ould-Amara, S.; Zadick, A.; Petit, E.; Chatenet, M.; Cretin, M.; Demirci, U. B. The

Highly Stable Aqueous Solution of Sodium Dodecahydro-Closo-Dodecaborate $Na_2B_{12}H_{12}$ as a Potential Liquid Anodic Fuel. *Appl. Catal., B* **2018**, 222, 1– 8 .

19. Miller, H. C., Miller, N. E., & Muetterties, E. L., Synthesis of polyhedral boranes. *J. Am. Chem. Soc.,* **1963,** 85(23), 3885-3886.

20. Hansen, B. R. S.; Paskevicius, M.; Li, H.-W.; Akiba, E.; Jensen, T. R. Metal boranes: Progress and applications. *Coord. Chem. Rev.* **2016,** 323, 60– 70.

21. He, L.; Li, H.-W.; Hwang, S.-J.; Akiba, E. Facile Solvent-Free Synthesis of Anhydrous Alkali Metal Dodecaborate $M_2B_{12}H_{12}$ (M = Li, Na, K) *J. Phys. Chem. C* **2014,** 118, 6084– 6089.

22. Caputo, R.; Garroni, S.; Olid, D.; Teixidor, F.; Surinach, S.; Baro, M. D., Can $Na_{(2)}[B_{(12)}H_{(12)}]$ be a decomposition product of $NaBH_{(4)}$? *Phys. Chem. Chem. Phys.* **2010,** 12, 15093– 15100.

23. Souza, D. H. P.; Moller, K. T.; Moggach, S. A.; Humphries, T. D.; D'Angelo, A. M.; Buckley, C. E.; Paskevicius, M. Hydrated Alkali-$B_{11}H_{14}$ Salts as Potential Solid-State Electrolytes. *J. Mater. Chem. A* **2021,** 9, 15027– 15037 .

24. Hagemann, H.; Cerny, R., Synthetic approaches to inorganic borohydrides. *Dalton Trans* **2010,** *39* (26), 6006-12.

25. Zhdanko, A.; Worp, B. A.; Lemaire, S., Coordination Chemistry of Borane in Solution: Application to a STING Agonist. *Eur. J. Org. Chem.* **2022,** *2022* (13).

26. Moury, R.; Gigante, A.; Hagemann, H. An Alternative Approach to the Synthesis of NaB_3H_8 and $Na_2B_{12}H_{12}$ for Solid Electrolyte Applications. *Int. J. Hydrogen Energy* **2017,** 42, 22417– 22421.

27. Verdal, N.; Her, J.-H.; Stavila, V.; Soloninin, A. V.; Babanova, O. A.; Skripov, A. V.; Udovic, T. J.; Rush, J. J., Complex high-temperature phase transitions in $Li_2B_{12}H_{12}$ and $Na_2B_{12}H_{12}$. *J. Solid State Chem.* **2014,** *212*, 81-91.

28. Chen, X.; Liu, X. R.; Wang, X.; Chen, X. M.; Jing, Y.; Wei, D., A safe and efficient synthetic method for alkali metal octahydrotriborates, unravelling a general mechanism for constructing the delta B_3 unit of polyhedral boranes. *Dalton Trans* **2021,** *50* (39), 13676-13679.

29. Chen, X.-M.; Ma, N.; Zhang, Q.-F.; Wang, J.; Feng, X.; Wei, C.; Wang, L.-S.; Zhang, J.; Chen, X., Elucidation of the Formation Mechanisms of the Octahydrotriborate Anion ($B_3H_8^-$) through the Nucleophilicity of the B–H Bond. *J. Am. Chem. Soc.* **2018,** *140* (21), 6718-6726.

For Table of Contents Only:

Abstract Graphic

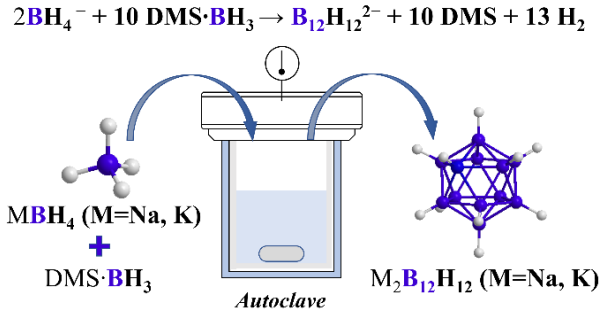

Synopsis:

A new facile synthetic method to obtain high purity $M_2B_{12}H_{12}$ (M= Na, K) in high yields has been developped, consisting of directly reacting the MBH_4 salts with $DMS{\cdot}BH_3$ in an autoclave. This approach paves the way to large scale synthesis of dodecaborates, and thus to the larger scope of their applications.